Diamond & Related Materials 88 (2018) 18–22

Contents lists available at ScienceDirect

Diamond & Related Materials

journal homepage: www.elsevier.com/locate/diamond

High surface area carbon materials derived from corn stalk core as electrode for supercapacitor

Kaifeng Yu[a], He Zhu[a], Hui Qi[b], Ce Liang[a,*]

[a] Key Laboratory of Automobile Materials, Ministry of Education, College of Materials Science and Engineering, Jilin University, Changchun 130025, PR China
[b] The Second Hospital of Jilin University, Changchun 130041, PR China

ARTICLE INFO

Keywords:
Activated carbon
Corn stalk core
Electrochemistry
Supercapacitor

ABSTRACT

The activated carbon materials from the corn stalk core raw materials were prepared through the carbonization and activation process and applied as electrode in supercapacitor. The biomass carbon materials activated under different temperatures were tested by cyclic voltammetry, electrochemical impedance spectroscopy and galvanostatic charge-discharge cycling method. The corn stalk core-derived material activated at 700 °C with the highest specific surface area (2349.89 $m^2 g^{-1}$) has exhibited the maximum specific capacitance of 140 $F g^{-1}$. Further detailed characterization and theoretical analysis have demonstrated that the corn stalk core derived activated carbon anode material can not only enhance the capacity of supercapacitor but also realize the comprehensive utilization of corn stalks.

1. Introduction

With the increasing energy consumption, it is urgent to search for sustainable and renewable energies. Considering the environmental problems brought by fossil fuels, the energy conservation and pollution reduction will be the significant factors in social and economic development. As a pollution-free "GREEN" energy storage system, the electrochemical supercapacitors combine both advantage of batteries and conventional capacitors, and have attracted much attention due to their potential applications ranging from mobile devices to electric vehicles [1, 2]. In recent years, researches in developing supercapacitors are underway to provide ideal power source with excellent power density coupled with rapid charge and discharge capabilities and long cycle life [3, 4].

Based on the energy storage mechanism, supercapacitors can be categorized into electrochemical double layer capacitors (EDLC) and faradic pseudocapacitors. The storage mechanism in EDLC is mainly based on the charged separation at electrode and electrolyte interface, while the faradic pseudocapacitors provide capacitor with the reversible faradic reactions occurring at the electrode surface [5, 6]. The most commonly used electrode materials in supercapacitors are conductive polymer, metal oxide and carbon materials, among them, the commercial applications of conductive polymer and metal oxide are limited owing to their small surface area and high cost.

As the earliest electrode applied in supercapacitors, carbon materials have lots of advantages such as low cost, high conductivity, controllable porous structure and high surface area [7–10]. Activated carbon (AC) [11–13], graphite [14, 15] and carbon nanotube [16] are common electrode materials in EDLC. At present activated carbons are widely used for capacitors according to its high porosity and high surface area that favors good charge accumulation at the interface with the electrolyte and therefore high capacitance can be tapped. In view of low cost and environmental protection, biomass wastes are great substitute for coal and petroleum and mainly studied as raw materials to prepare AC materials (ACs) [17, 18]. Huang et al. [19] prepared the activated carbon fibers (ACFs) using wood sawdust as raw materials, the ACFs showed outstanding electrochemical performance. Dechen Liu [20] prepared the rice husk-based activated carbon by KOH activation and the carbon materials possessed a specific surface area as high as 3263 $m^2 g^{-1}$. Corn stalk, as a kind of common biomass wastes, can be used to prepare electrode materials and applied in supercapacitors, which would solve the environment problem of burning stalks and make full use of resource. In addition, the corn stalk core (CSC) with sponge-like shape has abundant natural porous structure, which can be used to obtain ACs with high surface area and porous structure, and thus boost the capacity of supercapacitors when further used as electrode materials. Cao [21] prepared ACs using corn stalk as raw materials and exhibited the high capacitance of 323 $F g^{-1}$ at a current density of 0.1 $A g^{-1}$. However, the complex prepared procedure which introduced the metallic element has increased the cost and limited development. In this work, the ACs derived from CSC were prepared via carbonizing and activating procedure, which was simple and low cost.

* Corresponding author.
E-mail address: liangce@jlu.edu.cn (C. Liang).

https://doi.org/10.1016/j.diamond.2018.06.018
Received 15 March 2018; Received in revised form 15 June 2018; Accepted 20 June 2018
Available online 27 June 2018
0925-9635/

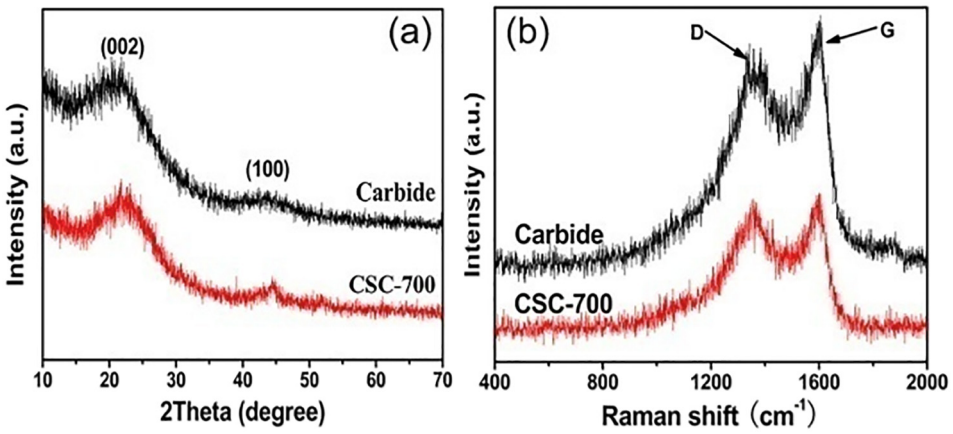

Fig. 1. XRD pattern (a) and Raman spectrum (b) of unactivated carbide and CSC-700.

The ACs activated at different temperatures were applied as electrode in supercapacitor. Moreover, electrochemical measurements were taken to evaluate the performance of various ACs and the optimal activated temperature was selected.

2. Experimental

2.1. Preparation of activated carbon materials

The activated carbon materials (ACs) for this work were synthesized as described follow. Firstly, the corn stalks core (CSC) was cleaned to remove the surface dirt, dried at 60 °C for 24 h and ground into a fine power by pulverizer. Secondly, the dried CSC was carbonized in the tube furnace at 400 °C for 2 h under nitrogen atmosphere with a heating rate of 2.5 °C min^{-1}. Then the obtained carbide was mixed with KOH solution at a mass ratio of 1:3 and dried at 60 °C for 24 h. Later, the dried mixture was heated again at 400 °C under nitrogen atmosphere and held for 30 min before being activated at 500–800 °C for 1 h with a heating rate of 5 °C min^{-1}. Finally, in order to remove the metal-oxide produced in the carbonized process, the obtained activated materials were further purified in 2 mol L^{-1} HCl solution within a water bath at 90 °C for 1 h and washed with deionized water until the solution was neutral, and then dried at 60 °C. The different activated temperature samples were denoted as CSC-500, CSC-600, CSC-700 and CSC-800, respectively.

2.2. Characterization of activated carbon materials

The morphologies and microstructures of ACs samples were observed by scanning electron microscopy (SEM) with a field-emission-scanning electron microscope (JEOL JSM-6700F) and transmission electron microscopy (TEM, JEOL JEM-2100F). Raman spectra were recorded on a Renishaw inVia instrument. X-ray diffraction (XRD) patterns were collected on a Bruker D8 Advance X-ray Diffractometer. The specific surface area and pore size distribution of the carbon materials were measured using nitrogen adsorption–desorption measurements (Micromeritics, ASAP 2420).

2.3. Preparation of electrodes

The working electrode was prepared by mixing the prepared activated materials (ACs), carbon black and polymer binder polyvinylidene fluoride (PVDF) in a 80:10:10 (wt%) ratio in *N*-methyl-2-pyrrolidone. The mixture was uniformly cast on pure nickel foam used as the current collectors and dried under vacuum at 120 °C for 12 h. The coating materials were covered on nickel foam with a surface area of (1 × 1) cm^2. The electrode was pressed under 50 MPa for 5 s. Moreover, in order to be fully soaked, the prepared electrodes were immersed with ethyl alcohol and potassium hydroxide solution for 24 h, respectively. In addition, the platinum electrode and calomel electrode were used as counter electrode and reference electrode, respectively. All the electrodes were dipped into 3 mol L^{-1} potassium hydroxide solution while testing the performance of supercapacitor.

2.4. Electrochemical measurements

In this work, electrochemical measurements were performed on a CHI660E electrochemical workstation. Cyclic voltammetry (CV) measurements were performed with a voltage window of −0.8 V to 0.2 V at different scan rates ranging from 10 mV s^{-1} to 100 mV s^{-1}. Galvanostatic charge-discharge cycling measurements were conducted with a voltage window of −0.8 V to 0.2 V at different current densities ranging from 0.5 A g^{-1} to 5 A g^{-1}. Electrochemical impedance spectroscopy (EIS) measurements were tested with the frequency ranging from 0.01 to 10,000 Hz. The specific capacitance was calculated using the following formula:

$$C_m = \frac{I\Delta t}{\Delta V}$$

In this formula, I is the discharge current density and Δt is the discharge time in the galvanostatic charge-discharge cycling measurements, ΔV is the range of voltage change.

3. Results and discussion

3.1. Characterization of carbon materials

The X-ray diffraction pattern of unactivated carbide and CSC-700 are displayed in Fig. 1(a). Curves possessed no evident sharp diffraction peaks, which indicated the amorphous carbon structure of the carbon materials. Two broad diffraction peaks located at 23° and 44° signified the characteristic peak of graphite (002) lattice plane that attributed to the interconnection and parallel stacking of flake graphite layers, while the (100) lattice suggested the hexagonal honeycomb structure contained in the pyrolytic carbon [22, 23]. Furthermore, the diffraction peak at 44° of CSC-700 was more prominent than that of unactivated carbide, which demonstrated the increasing of graphitization degree after activation.

As shown in Fig. 1(b), both samples exhibited a disorder-induced D-band (~1340 cm^{-1}) and in-plane vibrational G-band (~1590 cm^{-1}) in the Raman spectra, the former ascribed to the defections and disordered carbon in the graphitic structure, and the latter attributed to the vibration of sp2-bonded carbon atoms in a 2D hexagonal lattice. The ratio of intensity between D-band and G-band (ID/IG) reflected the degree of graphitization and the higher ratio represented the lower degree of

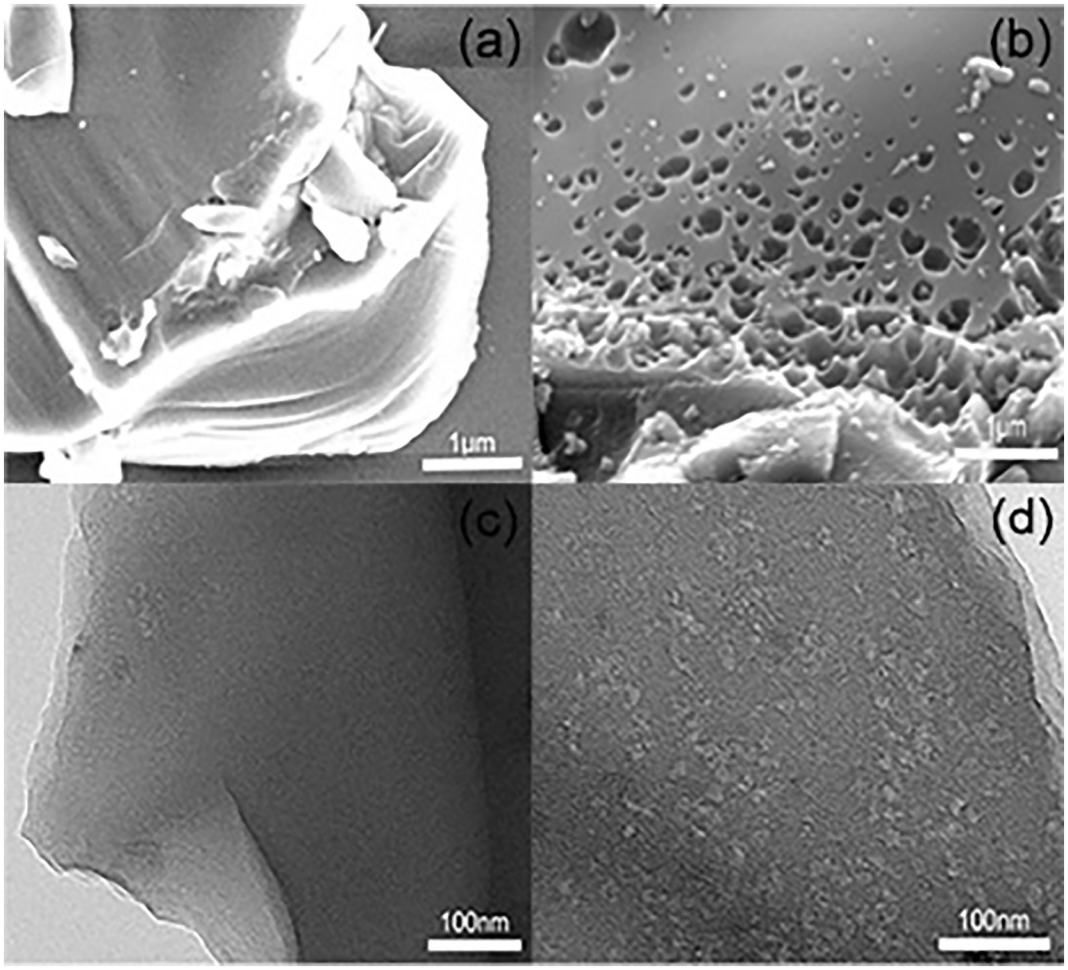

Fig. 2. (a) SEM image of unactivated carbide, (b) SEM image of CSC-700, (c) TEM image of unactivated carbide, (d) TEM image of CSC-700.

graphitization [24]. Thus, the CSC-700 (ID/IG = 0.94) had a higher degree of disorder compared with the unactivated carbide (ID/IG = 0.86). Combined with the SEM and TEM results, the CSC-700 with porous structure and higher degree of disorder possessed a higher surface area and will further enhance the capacity of the supercapacitor when used as the electrode.

The surface morphologies of unactivated carbide and CSC-700 characterized by SEM were shown in Fig. 2(a) and (b). It was obvious that the surface of carbide was fairly smooth and compact, and there were little fragments on the carbonaceous chunk from Fig. 2(a). However, the existence of abundant pores in CSC-700 had made the carbon structure unconsolidated, and a vast number of pieces appeared from Fig. 2(b). It had indicated that the activated process possesses significant function of opening pores and enlarging holes. The micromorphology and structure of unactivated carbide and CSC-700 were further observed through TEM and the results were shown in Fig. 2(c) and (d). The unactivated carbonaceous materials presented a sheet-like bulk structure with no evident pores inside, while the surface of CSC-700 appeared a plenty of traces corroded by potassium hydroxide through the activated process, which had increased the material specific surface area and pore size.

The nitrogen adsorption isotherm for CSC-700 was showed in the Fig. 3. According to the isotherms tendency of CSC-700, ACs presented both type-I and type-IV isotherms. Type-I isotherm indicated the existence of abundant microporous in the materials [25], which leaded to the high specific surface area of 2349.37 $m^2 g^{-1}$. The tiny hysteresis loop was the typical characteristic of type-IV isotherm and demonstrated the appearance of mesoporous. On the contrary, the BET surface

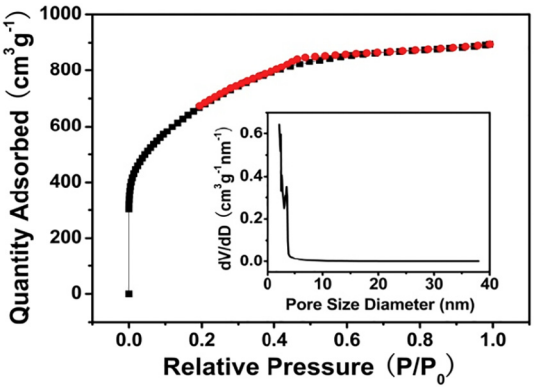

Fig. 3. Nitrogen adsorption-desorption isotherms and pore size distribution of CSC-700.

area value (only 35.65 $m^2 g^{-1}$) of CSCC had indicated the nonporous structure in carbide. According to the pore size distribution of CSC-700 shown in the Fig. 2, the distribution of pore size numerously concentrates on the 3 nm or so, which was facilitated to the transfer of electrolyte ion and enhanced the capacity of the electrode materials.

3.2. Electrochemical performance of activated carbons

The galvanostatic charge-discharge measurement could be used to test the electrochemical performance of supercapacitor. Different ACs prepared at various activation temperatures were used as electrode and

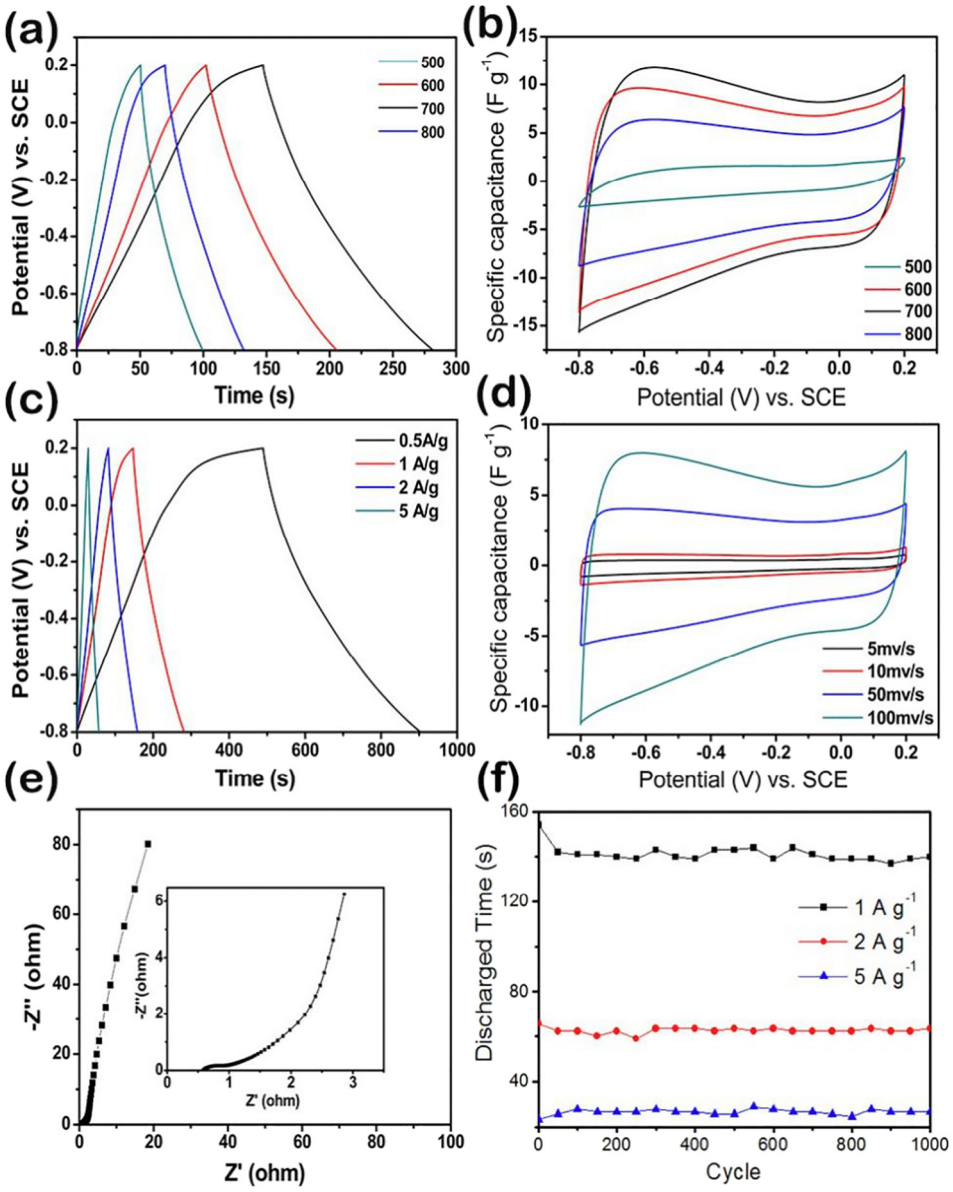

Fig. 4. Electrochemical performance of ACs as electrode in supercapacitor: (a) Charge-discharge curves of ACs at the current density of 1 A g^{-1}. (b) CV curves of ACs at the scan rate of 100 mV s^{-1}. (c) Charge-discharge curves of the CSC-700 at the different current density ranging from 0.5 to 5 A g^{-1}. (d) CV curves of the CSC-700 at the different scan rates ranging from 5 to 100 mV s^{-1}. (e) Nyquist plot based on the CSC-700 electrode. (f) Stability test of CSC-700 at the current density of 1 A g^{-1}, 2 A g^{-1} and 5 A g^{-1} for 1000 cycles, respectively.

tested. The results presented in Fig. 4(a). It was obvious that every curve seems symmetrical triangle at the current density of 1 A g^{-1}. For various carbon materials, the order of discharge time was CSC-500 < CSC-800 < CSC-600 < CSC-700, which corresponds to the specific capacitance order of 50 < 64 < 105 < 140 F g^{-1}, respectively. The porous structure formed gradually with the increasing of activated temperature, thus, CSC-700 electrode materials revealed the excellent electrochemical performance due to the porous structure, which profited to the transmission of electrolyte ions and provided vast absorbing sites for the ions. However, when the temperature was too high, the matrix of carbon would collapse gradually [26]. Therefore, the discharge time of CSC-700 was higher than CSC-800.

The cyclic voltammogram (CV) was also a typical mean to measure the electrochemistry performance level of supercapacitor. At the constant scan rate of 100 mV s^{-1}, the CV curves of different ACs were shown in Fig. 4(b). All quasi-rectangular shaped CV curves had indicated that the carbon materials were similar to the ideal electrode materials, and the area value of CV curves could reflect the capacity of supercapacitor. Among these corn stalk core-derived carbon materials, CSC-700 with the utmost curve area had possessed its excellent capacity, which was in accordance with the conclusion of galvanostatic charge-discharge measurement. Owing to the excellent electrochemical behavior, the CSC-700 sample was used to further test.

The Fig. 4(c) showed the galvanostatic charge-discharge curves of CSC-700 at the current density ranging from 0.5 A g^{-1} to 5 A g^{-1}. The discharge time decreased gradually with the increase of current density and the reduced percent was about 23%, this may result from that there was hardly any time for the electrolyte ions to enter and diffuse into the porosity of carbon materials. The CV curves of CSC-700 at different scan rates ranging from 10 mV s^{-1} to 100 mV s^{-1} were plotted in the Fig. 4(d). The rectangular shapes of CV curves were distorted gradually with the increasing scan rates. However, the CV curves remained quasi-rectangular shape at the high scan rate of 100 mV s^{-1}, it had indicated the excellent capacitor behavior of the electrode materials owing to the

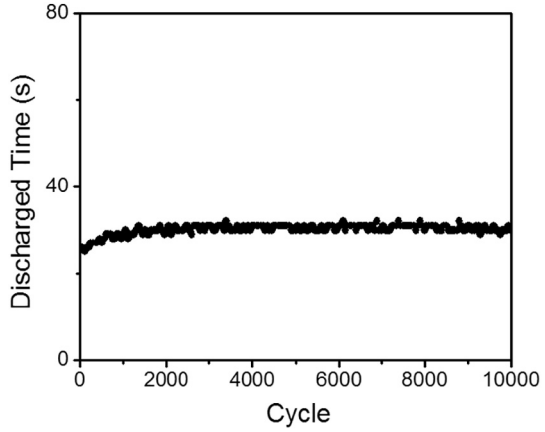

Fig. 5. Stability test of CSC-700 at the current density of 5 A g^{-1} for 10,000 cycles.

porous structure of samples.

Moreover, the electrochemical impedance spectra (EIS) of CSC-700 were obtained to further explore the electrochemical performance of ACs and the resistance of supercapacitor. The result was showed in Fig. 4(e) and the inset was the partial enlarged detail. A semicircle was observed in the high frequency region, which represented the charge transfer resistance (Rct) at the electrode-electrolyte interface. In addition, the small diameter of the semicircle represents the small charge transfer resistance due to the porous structure of the sample [27, 28]. The almost perpendicular line in the low-frequency region tilted with superior angles than 45° indicates a slight deviation from ideal capacitive behavior, and also the existence of a low diffusion resistance of ions within the electrode material. In summary, the ACs presented excellent electrochemical performance.

One merits of the supercapacitor was ultra-long cycle life, in order to evaluate the cycle performance, the sample of CSC-700 was further charged and discharged for 1000 cycles at current density of 1 A g^{-1}, 2 A g^{-1} and 5 A g^{-1}, respectively. As the Fig. 4(f) shown, the capacitance retained about 91% at the current density of 1 A g^{-1}, suggesting the excellent stabilized performance of the carbon materials. In addition, the capacitance retained about 96% even at the high current density, which indicated the remarkable rate performance. In order to further study the stability, the 10,000 cycles were tested at the current density of 5 A g^{-1}. As the Fig. 5 shown, the discharged time of CSC-700 was almost constant, which manifested the superior stability of ACs. Furthermore, the value increased in the initial stage can be attributed to the process of electrolyte immersing in the materials.

4. Conclusions

In this study, the activated carbon materials that used corn stalk core as raw materials and prepared at different activated temperature were applied to supercapacitor as electrode. With the highest surface area of 2349.89 $m^2 g^{-1}$, the CSC-700 exhibited an excellent capacitance of 140 F g^{-1} in the current density of 1 A g^{-1}. The synthesis temperature of CSC-700 was identified to the optimal activation temperature through further electrochemical measurements. The results proved by detailed characteristics and analysis have point out that the corn stalk core derived activated carbon anode material could not only enhance the capacity of supercapacitor but also realize the comprehensive utilization of corn stalks.

Acknowledgements

This work was financially supported by National Science Foundation of China (51275203); the Project of Education Department of Jilin Province (JJKH20180130KJ); the Key Scientific and Technological Project of Jilin Province (20140204052GX, 20180201074GX); China Postdoctoral Science Foundation (2017M611321).

References

[1] E. González, J.A. Goikolea, R. Mysyk Barrena, Review on supercapacitors: technologies and materials, Renew. Sust. Energ. Rev. 58 (2016) 1189–1206.
[2] L.L. Zhang, X.S. Zhao, Carbon-based materials as supercapacitor electrodes, Chem. Soc. Rev. 38 (2009) 2520–2531.
[3] P. Simon, Y. Gogotsi, B. Dunn, Where do batteries end and supercapacitors begin, Science 343 (2014) 1210–1211.
[4] G.P. Wang, L. Zhang, J.J. Zhang, A review of electrode materials for electrochemical supercapacitors, Chem. Soc. Rev. 41 (2012) 797–828.
[5] A. Ghosh, Y.H. Lee, Carbon-based electrochemical capacitor, ChemSusChem 5 (2012) 480–499.
[6] K.S. Xia, Q.M. Gao, J.H. Jiang, J. Hu, Hierarchical porous carbon with controlled micropores and mesopores for supercapacitor electrode materials, Carbon 46 (2008) 1718–1726.
[7] M.M. Sk, C.Y. Yue, K. Ghosh, R.K. Jena, Review on advance in porous nanostructured nickle oxides and their composite electrodes for high-performance supercapacitors, J. Power Sources 308 (2016) 121–140.
[8] C. Long, J. Zhuang, Y. Xiao, M. Zheng, H. Hu, H. Dong, B. Lei, H. Zhang, Y. Liu, Nitrogen-doped porous carbon with an ultrahigh specific surface area for superior performance supercapacitors, J. Power Sources 310 (2016) 145–153.
[9] L.Q. Li, H.B. Yang, J. Yang, L.P. Zhang, J.W. Miao, Y.F. Zhang, C. Sun, W. Huang, X.C. Dong, B. Liu, Hierarchical carbon@Ni_3S_2@MoS_2 double core-shell nanorods for high-performance supercapacitors, J. Mater. Chem. A 4 (2016) 1319–1325.
[10] Q. Wang, J. Yan, Y. Wang, T. Wei, M. Zhang, X. Jing, Z. Fan, Three-dimensional flower-like and hierarchical porous carbon materials as high-rate performance electrodes for supercapacitors, Carbon 67 (2014) 119–127.
[11] K.L. Van, T.T.L. Thi, Activated carbon derived from rice husk by NaOH activation and its application in supercapacitor, Prog. Nat. Sci.: Mater. Int. 24 (2014) 191–198.
[12] G. Yuan, F. Yin, Y. Zhao, Z. Bakenov, G. Wang, Y. Zhang, Corn stalk-derived activated carbon with a stacking sheet-like structure as sulfur cathode supporter for lithium/sulfur batteries, Ionics 22 (2016) 63–69.
[13] S.G. Lee, K.H. Park, W.G. Shim, M.S. Balathanigaimani, H. Moon, Performance of electrochemical double layer capacitors using highly porous activated carbons prepared from beer lees, J. Ind. Eng. Chem. 17 (2011) 450–454.
[14] Y.H. Hwang, S.M. Lee, Y.J. Kim, Y.H. Kahng, K. Lee, A new approach of structural and chemical modification on graphene electrodes for high-performance supercapacitors, Carbon 100 (2016) 7–15.
[15] J. Xu, Z. Tan, W. Zeng, G. Chen, S. Wu, Y. Zhao, K. Ni, Z. Tao, M. Ikram, H. Ji, Y. Zhu, Hydrothermal conversion of biomass waste to activated carbon with high porosity: a review, Adv. Mater. 28 (2016) 5222–5228.
[16] J. Jiang, L. Li, Y. Liu, S. Liu, M. Xu, J. Zhu, Uniform implantation of CNTs on total activated carbon surfaces: a smart engineering protocol for commercial supercapacitor applications, Nanotechnology 28 (2017) 145402.
[17] A. Jain, R. Balasubramanian, M.P. Srinivasan, Hydrothermal conversion of biomass waste to activated carbon with high porosity: a review, Chem. Eng. J. 283 (2016) 789–805.
[18] Y.Q. Zhao, M. Lu, P.Y. Tao, Y.J. Zhang, X.T. Gong, Z. Yang, G.Q. Zhang, H.L. Li, Hierarchically porous and heteroatom doped carbon derived from tobacco rods for supercapacitors, J. Power Sources 307 (2016) 391–400.
[19] Y. Huang, L. Peng, Y. Liu, G. Zhao, J.Y. Chen, G. Yu, Biobased nano porous active carbon fibers for high-performance supercapacitors, ACS Appl. Mater. Interfaces 8 (2016) 15205–15215.
[20] D. Liu, W. Zhang, H. Lin, Y. Li, H. Lu, Y. Wang, A green technology for the preparation of high capacitance rice husk-based activated carbon, J. Clean. Prod. 112 (2016) 1190–1198.
[21] Y. Cao, K. Wang, X. Wang, Z. Gu, Q. Fan, W. Gibbons, J.D. Hoefelmeyer, P.R. Kharel, M. Shrestha, Hierarchical porous activated carbon for supercapacitor derived from corn stalk core by potassium hydroxide activation, Electrochim. Acta 212 (2016) 839–847.
[22] M. Liu, L. Gan, W. Xiong, F. Zhao, X. Fan, D. Zhu, Z. Xu, Z. Hao, L. Chen, Nickel-doped activated mesoporous carbon microspheres with partially graphitic structure for supercapacitors, Energy Fuel 27 (2013) 1168–1173.
[23] Y.J. Hwang, S.K. Jeong, J.S. Shin, K.S. Nahm, A.M. Stephan, High capacity disordered carbons obtained from coconut shells as anode materials for lithium batteries, J. Alloys Compd. 448 (2008) 141–147.
[24] S.W. Han, D.W. Jung, J.H. Jeong, E.S. Oh, Effect of pyrolysis temperature on carbon obtained from green tea biomass for superior lithium ion battery anodes, Chem. Eng. J. 254 (2014) 597–604.
[25] T.D. Nguyen, J.K. Ryu, S.N. Bramhe, T.N. Kim, Performance of electric double layers capacitor using activated carbon materials from rice husk as electrodes, Korean J. Mater. Res. 23 (2013) 643–648.
[26] A.C. Lua, T. Yang, Effect of activation temperature on the textural and chemical properties of potassium hydroxide activated carbon prepared from pistachio-nut shell, J. Colloid Interface Sci. 274 (2004) 594–601.
[27] Q. Ruibin, H. Zhongai, Y. Yuying, L. Zhimin, A. Ning, R. Xiaoying, H. Haixiong, W. Hongying, Monodisperse carbon microspheres derived from potato starch for asymmetric supercapacitors, Electrochim. Acta 167 (2015) 303–310.
[28] X. He, P. Ling, J. Qiu, M. Yu, X. Zhang, C. Yu, M. Zheng, Efficient preparation of biomass-based mesoporous carbons for supercapacitors with both high energy density and high power density, J. Power Sources 240 (2013) 109–113.